Quasi-one-dimensional Bose-Einstein condensates in nonlinear lattices

Luca Salasnich

Dipartimento di Fisica e Astronomia “Galileo Galilei” and CNISM, Università di Padova

Sevilla, July 12, 2012

Collaboration with:
Boris A. Malomed (Tel Aviv University)

Summary

- Modeling a quasi-1D BEC in nonlinear lattice
- Gaussian variational approach
- Nonpolynomial Schrodinger equation (NPSE)
- Density profiles of bright solitons
- Collective oscillations of bright solitons
- Stability diagram of bright solitons
- Immobility of bright solitons
- Conclusions

Modeling quasi-1D BEC in nonlinear lattice

We consider a dilute BEC of atoms with mass m confined in the transverse plane by the isotropic harmonic-oscillator potential with frequency $\omega_\perp$,

$$V(x, y) = \frac{1}{2} m\omega_\perp^2 \left(x^2 + y^2\right) . \quad (1)$$

The corresponding adimensional 3D Gross-Pitaevskii equation (GPE) is

$$i\frac{\partial \psi}{\partial t} = \left[-\frac{1}{2}\nabla^2 + \frac{1}{2}\left(x^2 + y^2\right) + 2\pi g(z)|\psi|^2\right]\psi, \quad (2)$$

where lengths are in units of $a_\perp = \sqrt{\hbar/(m\omega_\perp)}$ and energies in units of $\hbar\omega_\perp$. The interaction strength in Eq. (2) is

$$g(z) = 2(N-1)a_s(z)/a_\perp , \quad (3)$$

where N is the number of atoms and $a_s(z)$ the space-dependent scattering length of the inter-atomic potential. In our model we consider a nonlinear lattice (NL) given by

$$g(z) = g_1 \cos(2kz) , \quad (4)$$

where $g_1 < 0$ is the depth of the NL potential.

Gaussian variational approach (GVA)

We notice that the GPE can be derived from the Lagrangian density,

$$\mathcal{L} = \frac{i}{2}(\psi^* \frac{\partial \psi}{\partial t} - \psi \frac{\partial \psi^*}{\partial t}) - \frac{1}{2}|\nabla \psi|^2 - \frac{1}{2}\left(x^2 + y^2\right)|\psi|^2 - \pi g(z)|\psi|^4 \quad (5)$$

and make use of a time-dependent Gaussian ansatz,

$$\psi\left(\mathbf{r}, t\right) = \frac{\exp\left\{-\frac{1}{2}\left[\frac{r_\perp^2}{\sigma_\perp^2(t)} + \frac{z^2}{\sigma_\parallel^2(t)}\right] + i\beta_\perp(t) r_\perp^2 + i\beta_\parallel(t) z^2\right\}}{\pi^{3/4}\sigma_\perp(t)\sqrt{\sigma_\parallel(t)}}, \quad (6)$$

where $r_\perp^2 \equiv x^2 + y^2$, and $\sigma_\perp(t)$, $\sigma_\parallel(t)$ and $\beta_\perp(t)$, $\beta_\parallel(t)$ are time-dependent variational parameters. This wave function is an exact one for non-interacting bosons ($g = 0$) in the harmonic trap.

Gaussian variational approach (GVA)

Inserting the ansatz into Lagrangian density (5) and performing the spatial integration, we arrive at the effective Lagrangian,

$$
\begin{aligned}
L &= -\frac{1}{2}\Big[\big(2\dot{\beta}_\perp \sigma_\perp^2 + \frac{1}{\sigma_\perp^2} + 4\sigma_\perp^2\beta_\perp^2 + \sigma_\perp^2\big) && (7)\\
&+ \big(\dot{\beta}_\parallel \sigma_\parallel^2 + \frac{1}{2\sigma_\parallel^2} + 2\sigma_\parallel^2\beta_\parallel^2\big) + \frac{g_0 + g_1 e^{-k^2\sigma_\parallel^2/2}}{\sqrt{2\pi}\ \sigma_\perp^2\sigma_\parallel}\Big], && (8)
\end{aligned}
$$

with the overdot standing for time derivatives. The respective Euler-Lagrange equations take the form of

$$
\begin{aligned}
\beta_\perp &= -\frac{\dot{\sigma}_\perp}{2\sigma_\perp}\ , && (9)\\
\beta_\parallel &= -\frac{\dot{\sigma}_\parallel}{2\sigma_\parallel}\ , && (10)\\
\ddot{\sigma}_\perp + \sigma_\perp &= \frac{1}{\sigma_\perp^3} + \frac{g_0 + g_1 e^{-k^2\sigma_\parallel^2/2}}{\sqrt{2\pi}\ \sigma_\perp^3\sigma_\parallel}\ , && (11)\\
\ddot{\sigma}_\parallel &= \frac{1}{\sigma_\parallel^3} + \frac{g_0 + g_1 e^{-k^2\sigma_\parallel^2/2}(1 + k^2\sigma_\parallel^2)}{\sqrt{2\pi}\ \sigma_\perp^2\sigma_\parallel^2}\ . && (12)
\end{aligned}
$$

Gaussian variational approach (GVA)

Next, we look for stationary configurations, i.e. $\dot{\sigma}_\perp = \dot{\sigma}_\parallel = \ddot{\sigma}_\perp = \ddot{\sigma}_\parallel = 0$, which yields

$$\beta_\perp = 0 \,, \tag{13}$$

$$\beta_\parallel = 0 \,, \tag{14}$$

$$\sigma_\perp = \frac{1}{\sigma_\perp^3} + \frac{g_0 + g_1 e^{-k^2\sigma_\parallel^2/2}}{\sqrt{2\pi}\; \sigma_\perp^3 \sigma_\parallel} \,, \tag{15}$$

$$0 = \frac{1}{\sigma_\parallel^3} + \frac{g_0 + g_1 e^{-k^2\sigma_\parallel^2/2}(1 + k^2\sigma_\parallel^2)}{\sqrt{2\pi}\; \sigma_\perp^2 \sigma_\parallel^2} \,. \tag{16}$$

The last two equations can be solved numerically.
Further, low-energy excitations of the condensate around the stationary state are represented by small oscillations of variables $\sigma_\perp(t)$ and $\sigma_\parallel(t)$ around the stationary configurations.

Nonpolynomial Schrödinger equation (NPSE)

A more accurate description is obtained by using the following ansatz

$$\psi(\mathbf{r},t) = \frac{1}{\sqrt{\pi}\sigma(z,t)} \exp\left[-\frac{x^2+y^2}{2\sigma(z,t)^2}\right] f(z,t). \tag{17}$$

Substituting ansatz (17) into Lagrangian density (5), performing the integration over x and y, and omitting spatial derivatives of the transverse width, we derive the respective Lagrangian density

$$\bar{\mathcal{L}} = \frac{i}{2}\left(f^*\frac{\partial f}{\partial t} - f\frac{\partial f^*}{\partial t}\right) - \frac{1}{2}\left|\frac{\partial f}{\partial z}\right|^2 - \frac{1}{2}\left(\frac{1}{\sigma^2}+\sigma^2\right)|f|^2 - \frac{1}{2}g(z)\frac{|f|^4}{\sigma^2} . \tag{18}$$

Varying it with respect to $f^*(z,t)$ and $\sigma(z,t)$ gives rise to the system of Euler-Lagrange equations

$$i\frac{\partial f}{\partial t} = \left[-\frac{1}{2}\frac{\partial^2}{\partial z^2} + \frac{1}{2}\left(\frac{1}{\sigma^2}+\sigma^2\right) + g(z)\frac{|f|^2}{\sigma^2}\right] f , \tag{19}$$

$$\sigma^4 = 1 + g(z)|f|^2 , \tag{20}$$

Nonpolynomial Schrödinger equation (NPSE)

Inserting Eq. (20) into Eq. (19), we obtain the NPSE for the axial wave function, but with the z-dependent interaction strength, $g(z)$:

$$i\frac{\partial f}{\partial t} = \Big[-\frac{1}{2}\frac{\partial^2}{\partial z^2} + \frac{1+(3/2)g(z)|f|^2}{\sqrt{1+g(z)|f|^2}} \Big] f \ . \tag{21}$$

In the weak-coupling regime, i.e., $|g(z)|\,|f(z,t)|^2 \ll 1$, one can expand NPSE, Eq. (21), arriving at the cubic-quintic NLSE

$$i\frac{\partial f}{\partial t} = \Big[-\frac{1}{2}\frac{\partial^2}{\partial z^2} + 1 + g(z)|f|^2 + \frac{3}{8}g(z)^2|f|^4 \Big] f \ . \tag{22}$$

On the other hand, in the strong-coupling regime, $g(z)|f(z,t)|^2 \gg 1$ (which is relevant only for the repulsive sign of the nonlinearity, $g > 0$), the NPSE amounts to the NLSE with the quadratic nonlinearity:

$$i\frac{\partial f}{\partial t} = \Big[-\frac{1}{2}\frac{\partial^2}{\partial z^2} + \frac{3}{2}\sqrt{g(z)}|f| \Big] f \ . \tag{23}$$

Density profiles of bright solitons

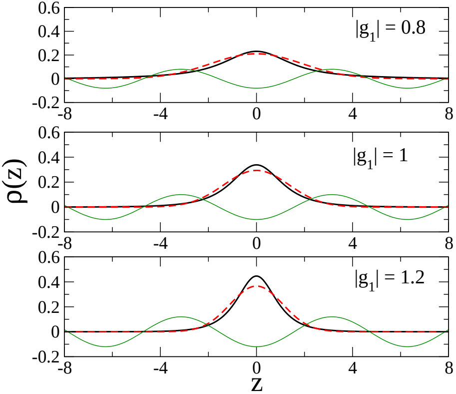

Figure: Typical examples of axial density $\rho(z) \equiv |f(z)|^2$ of stable bright solitons. The solid and dashed lines display the results produced by the NPSE and GVA,respectively, for three different values of the interaction strength $|g_1|$, fixing $k = 0.5$ and $g_1 < 0$. Here the green sinusoidal line represents the periodic modulation function of the local nonlinearity. [**Adapted from: LS and B.A. Malomed, JPB 45, 055302 (2012)**]

Collective oscillations of bright solitons

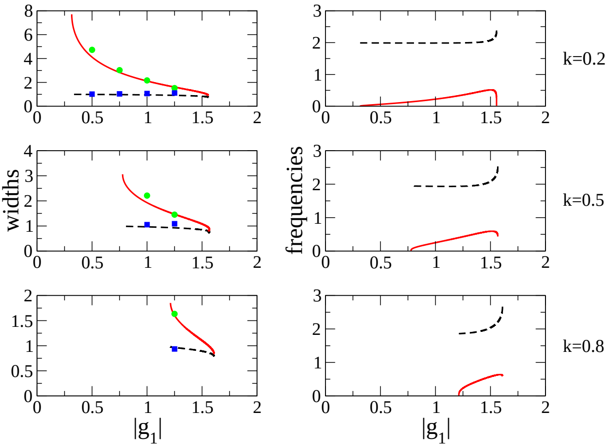

Figure: **Left panels**: transverse and axial widths, $\sigma_\perp$ and $\sigma_\parallel$ (dashed and solid lines, respectively) of stable bright solitons, vs $|g_1|$, with $g_1 < 0$. **Right panels**: frequencies Ω_1 and Ω_2 (dashed and solid lines) of collective excitations vs. $|g_1|$. Curves: GVA. Symbols: NPSE. [**Adapted from: LS and B.A. Malomed, JPB 45, 055302 (2012)**]

Stability diagram of bright solitons

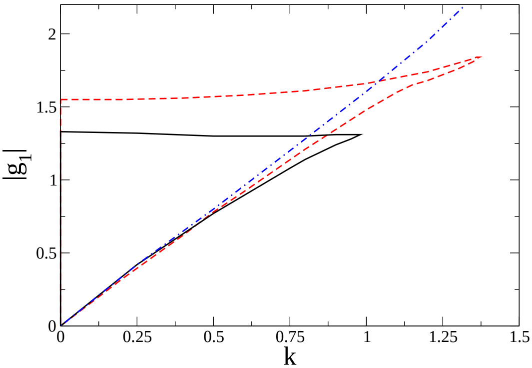

Figure: The stability diagram for the solitons in the plane of wavenumber k and strength $|g_1|$ of the NL, with $g_1 < 0$ The solitons are stable between the dashed lines, according to GVA, and between the solid lines, according to the NPSE. The dot-dashed line is the lower bound predicted by the one-dimensional cubic Gross-Pitaevskii equation. [**Adapted from: LS and B.A. Malomed, JPB 45, 055302 (2012)**]

Immobility of bright solitons

The mobility of solitons trapped in the NL can be tested by applying a kick to initially quiescent solitons.
For this purpose, NPSE was simulated with initial condition

$$f(z, t = 0) = f_{\mathrm{sol}}(z)\ e^{ivz}\ , \qquad (24)$$

where v is the magnitude of kick, i.e., the initial velocity imparted to soliton $f_{\mathrm{sol}}(z)$, which was produced by means of the imaginary-time simulations of the same NPSE.

Immobility of bright solitons

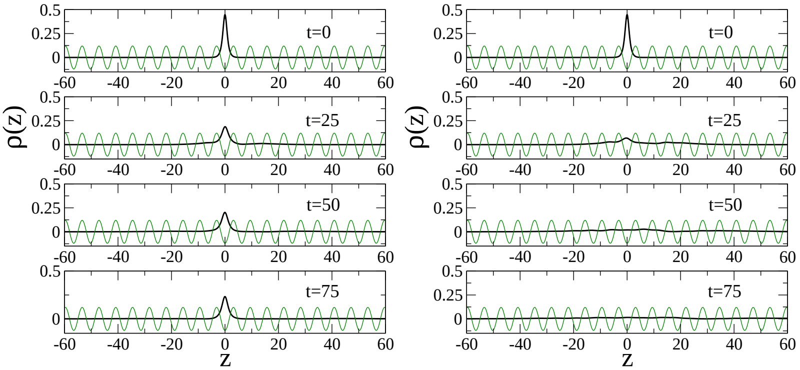

Figure: The evolution of the kicked soliton with initial velocities $v = 0.4$ (**left**) and $v = 0.6$ (**right**). Axial density $\rho(z)$ is plotted at different values of real time t, as obtained from simulations of NPSE. Here, $g_1 = -1.2$ and $k = 0.5$ are fixed. [**Adapted from: LS and B.A. Malomed, JPB 45, 055302 (2012)**]

Immobility of bright solitons

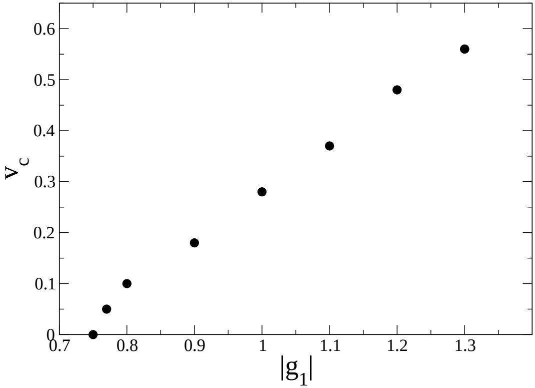

Figure: The critical velocity, v_c, for the destruction of the kicked soliton versus the strength of the nonlinear lattice, $|g_1|$. Here, $k = 0.5$ if fixed, as before. [**Adapted from: LS and B.A. Malomed, JPB 45, 055302 (2012)**]

Conclusions

- Our main result is the stability domain for bright solitons in the plane of the NL strength and wavenumber. We have obtained it with both GVA and NPSE.
- The usual 1D cubic Gross-Pitaevskii equation (1D GPE) with the NL does not produce adequate results, as it does not give rise to the collapse, which is the most important stability-limiting factor.
- Another difference with respect to 1D GPE: bright solitons are immobile in the framework of the NPSE with NL. The kick applied to the soliton either leaves it pinned, or, eventually, destroys it.